



Fréedericksz transition on a phenomenological model for a nematic inhomogeneous superfluid in presence of an electric field

Diego García Ovalle ^a, Juan Pablo Borgna ^{b,*}, Mariano De Leo ^c

^a Faculty of Physics, Pontificia Universidad Católica de Chile, Avda. Vicuña Mackenna 4860, Santiago, Chile

^b ICIFI (CONICET) - Applied Mathematics Center, Universidad de San Martín, Argentina

^c INMABB (CONICET) - Departamento de Matemática, Universidad Nacional del Sur, Argentina

ARTICLE INFO

Article history:

Received 31 May 2020

Received in revised form 28 July 2020

Accepted 26 August 2020

Available online 1 September 2020

Communicated by D. Pelinovsky

Keywords:

Nematic superfluid

Fréedericksz transition

First eigenvalue

ABSTRACT

In this article we derive a Ginzburg–Landau energy functional for a nematic inhomogeneous superfluid in presence of an electric field. The molecules occupy an infinite cylinder Ω with cross section D . We suppose vacuum in $\mathbb{R}^3 \setminus \Omega$, with the possibility that an external electric field can be applied parallel to D . The Helmholtz free energy is obtained by taking the London limit of a Ginzburg–Landau nematic superconducting model in absence of magnetic fields, and by including an appropriate contribution of the electric potential energy. We show that the critical parameter inside Ω , which defines the Fréedericksz transition on the molecular alignment, is not only influenced by the effects of the electric field in the sample, but also by the additional contribution of the superfluid current. We take a particular solution for the Ginzburg–Landau equations, where the superfluid phase does not have circulation. Then, we demonstrate that the corresponding Fréedericksz threshold can be calculated, on an arbitrary domain, by using the notion of the first positive eigenvalue of the Laplacian. This eigenvalue depends on the chosen geometry and the boundary conditions on the nematic phase in the sample. Next, we apply our results in an infinite slab and in an infinite cylinder with circular cross section, where the nematic superfluid system is subjected to Dirichlet or Neumann boundary conditions in each case. We deduce a modified Fréedericksz threshold, for each configuration mentioned before, in a uniform electric field. In these instances we notice the remarkable fact that, for specific values and regimes of the intrinsic parameters, the critical fields are different than the ones obtained in the pure nematic case. Finally, we also study a Fréedericksz type threshold in a long hollow cylinder with uniform charge density, where molecules are reoriented by the electric field produced only by the internal charges of the sample. This setting suggests that, if molecules are oriented radially at the boundary of the region, a Fréedericksz type threshold appears in order to maintain the radial molecular distribution, which varies with the typical radii of the domain.

© 2020 Elsevier B.V. All rights reserved.

1. Introduction

The angle of the molecules of a nematic liquid crystal is measured referencing an axis, which is characterized by a unitary director vector \hat{n} . This crystal is considered as uniaxial due to the rotational symmetry of its components [1]. Nematicons tend to be aligned parallel to an electromagnetic field, depending on the optical anisotropy of the sample. This effect is called Fréedericksz transition [2], which is typically defined by the magnitude of the applied field. In fact, the applied field strength plays the role of a critical parameter for the transition in nematic liquid crystals. In this framework, it has been proved experimentally that the

electric field has a deeper influence than the magnetic field in the molecular alignment. The range of experimental values for the electric permittivities is larger than the range of magnetic permeabilities for these materials [3]. Nevertheless, the mean orientational order can be strongly affected by the magnetic field in ferromagnetic liquid crystals, which are formed by diluted magnetic particles. The Fréedericksz transition of these materials can be different from the usual second order phase transition, and their properties have called the attention of both theoretical [4] and experimental [5] community.

On the other hand, superfluidity is an effect related to a phase transition where particles move without friction. Superconductivity represents a similar situation, but particles move without resistivity [6]. In both phenomena, the phase transition is related to a spontaneous rotational symmetry breaking, where the mass flux (magnetic flux) around a closed curve is quantized. Topological defects could appear in the contexts mentioned before, where

* Corresponding author.

E-mail addresses: ddgarcia@uc.cl (D. García Ovalle), jpborgna@unsam.edu.ar (J.P. Borgna), mariano.deleo@uns.edu.ar (M. De Leo).

the order parameters that describe the phase transitions have singularities such as (superfluid or superconducting) vortices or disclinations.

In this context, we construct a phenomenological model for nematic superfluids in presence of an electric field, based on the groundbreaking Ginzburg–Landau formalism. Previous works confirm theoretical [7] and experimental [8] interest on nematic superfluids, for example, in the problem of interacting bosons for frustrated lattices. Several authors have worked on models that combine nematicity with an electric field, even in the formation of optical solitons in nematic media [9–11].

We start by modifying an energy functional theory for a nematic superconductor [12], by taking into account a limit without magnetic fields and by adding a suitable term for the electric potential energy to the theory. These modifications allow us to explore the appearance of a Fréedericksz transition on different nematic superfluid samples, where we can compare the results with a pure nematic situation. Nematic superconductors are conjectured to exist among novel materials, for example, in the pseudo gap regime of high T_C superconductors. They are distinguished by a gauge and a rotational spontaneous symmetry breaking. Bulk thermodynamic evidences support the existence of these materials in 2017 [13], which were confirmed in 2018 [14]. From a theoretical point of view, a phenomenological Ginzburg–Landau theory was proposed from the simplest Pair Density Wave (PDW) state [15] and the Mc-Millan–de Gennes theory, and it explores the coupling between superconductivity and nematicity as a fluctuating metric [16]. A further research of Barci et al. in 2016 [12] suggests a simplified model for nematic superconductivity in the Ginzburg–Landau formalism.

According to Barci et al. in 2016 [12], the Ginzburg–Landau free energy per unit length of a two dimensional nematic superconducting sample is given by

$$F = \int_{\Omega} \left(a|\psi|^2 + \frac{b|\psi|^4}{2} + t|Q|^2 + \frac{u|Q|^4}{2} + v|\psi|^2|Q|^2 \right) d^2x + \int_{\Omega} \left(\alpha_s |\vec{D}\psi|^2 + \alpha_n |\vec{\nabla}Q|^2 + \frac{|\vec{\nabla} \times \vec{A}|^2}{8\pi} \right) d^2x + \int_{\Omega} \frac{2\alpha_s \Lambda S}{S_m} \left(|\hat{n} \cdot \vec{D}\psi|^2 - \frac{|\vec{D}\psi|^2}{2} \right) d^2x, \quad (1)$$

where ψ is the superconducting order parameter, Q is the nematic order parameter and \vec{A} is the magnetic vector potential. The magnetic field satisfies the fundamental relation $B = \vec{\nabla} \times \vec{A}$ and ψ couples minimally with \vec{A} through the covariant derivative $\vec{D} = \vec{\nabla} - iq_*\vec{A}$, with q_* the effective charge of the model. We also define $\hat{n}(\alpha) = \sin\alpha\hat{x} + \cos\alpha\hat{z}$ as the molecular director in a standard cartesian basis, where α is the nematic phase. For the first line of Eq. (1), we observe the usual expansion of the order parameters in theories of second order phase transitions, where a , b , t and u are intrinsic parameters that depend on temperature. Besides, it also includes an interaction term with strength v that couples the mean density of superconducting electrons $|\psi|^2$ and the mean density of nematic particles $|Q|^2$. For the second line of Eq. (1), we have the magnetic energy and the kinetic energy contributions of the nematic parameter and the superconducting parameter. Here, α_s is the superconducting stiffness and α_n is its counterpart for nematicity. The third line in Eq. (1) is the energetic contribution related to the fluctuating metric, where Λ is any small real number that represents its typical size.

We set $Q = S \exp 2i\alpha$ and $\psi = \rho \exp i\theta$, where θ is the superconducting phase, and we take the London limit by neglecting spatial fluctuations in Q and ψ . For this reason, we assume $S = S_m$ and $\rho = \rho_m$, i.e., their values in the homogeneous case (in fact, they can be approximated in the weak coupling

limit [12]). Therefore, if we consider a uniaxial material in the long cylindrical region $\Omega \subseteq \mathbb{R}^3$ of cross section $D \subseteq \mathbb{R}^2$, the Helmholtz free energy functional per unit length is

$$F_L = \int_D \left\{ \rho_s |\vec{\nabla}\theta + q_*\vec{A}|^2 + \lambda (\hat{n} \cdot (\vec{\nabla}\theta + q_*\vec{A}))^2 \right\} d^2x + \int_D \left\{ K |\vec{\nabla}\alpha|^2 + \frac{|\vec{\nabla} \times \vec{A}|^2}{8\pi} \right\} d^2x. \quad (2)$$

The set of intrinsic parameters (ρ_s , λ , K) have dimensions of energy per unit length, which are given by $\rho_s = \alpha_s \rho_m^2 (1 - \Lambda)$, $K = 4\alpha_n S_m^2$ and $\lambda = 2\alpha_s \rho_m^2 \Lambda$ [12]. We notice that the limit $\vec{A} = 0$ can represent both a nematic inhomogeneous superfluid or a bulk superconductor. If molecules are in presence of an electric field \vec{E} , our model cannot be interpreted as a nematic bulk superconductor since London equations [17] cannot be satisfied in the classical limit. We take into account a long cylindrical geometry for different cross sections. If we add the electric term to the energy functional, our chosen geometries can lead us to perform an analysis of Fréedericksz type transitions [2]. Moreover, this study can be useful for further applications, for instance, in more effective LCD devices.

Our article is organized as follows: In Section 2, we develop the fundamental structure of the model by defining the Helmholtz free energy per unit length (Section 2.1) and the Ginzburg–Landau equations (Section 2.2). In Section 2.3 we present a particular solution that relates the superfluid phase and the electric potential, on the primary supposition that the superfluid current does not circulate. In the next subsections we take this solution to study the Fréedericksz transition in two different configurations of the electric field \vec{E} . In Section 3.1 we present an alternative technique that computes the Fréedericksz transition by using the first eigenvalue of the Laplacian. In the general framework, the model shall be given by an elliptic operator stemmed from the first variation of the free energy. In Sections 3.2–3.3 we assume \vec{E} as a uniform electric field applied on two different geometries Ω , with cross sections given by an infinite slab and a disk. In Section 4 we consider that \vec{E} is a radial electric field centered in a long hollow cylinder, with an annulus as its cross section. In each case, we conclude that the superfluid current and the electric field determine the critical parameter for the Fréedericksz transition. Besides, we calculate the corresponding Fréedericksz thresholds for each instance. We add plots of the effective threshold in the uniform electric field case and in the radial electric field case as a function of relevant variables. We also include complementary graphics to illustrate the deviation on the molecular alignment, in the uniform electric field case, for the chosen domains.

2. Fundamentals of the model

2.1. Helmholtz free energy

Let us consider the Helmholtz free energy per unit length defined in Eq. (2) and assume that $\vec{A} = 0$. The contribution of \vec{E} to the energy functional consists of a known term in the literature [3,18] and the electrical work on the nematic superfluid molecules [19]:

$$F_E = \int_D (q_* \rho_m^2 \phi) d^2x - \int_{\mathbb{R}^2} \left(\frac{(\epsilon \vec{E}) \cdot \vec{E}}{2} \right) d^2x, \quad (3)$$

where ρ_m^2 is the absolute square of the superfluid order parameter in D . This also represents the mean density of superfluid molecules. $\phi(\vec{x})$ is the electric potential of the system, which we assume that satisfies the fundamental relation $\vec{E} = -\vec{\nabla}\phi$, and ϵ is

the electric permittivity tensor. Since the region Ω is occupied by a uniaxial material, this tensor can be expressed as follows [18]:

$$\epsilon = \begin{pmatrix} \epsilon_{\perp} & 0 & 0 \\ 0 & \epsilon_{\perp} & 0 \\ 0 & 0 & \epsilon_{\parallel} \end{pmatrix}, \quad (4)$$

where ϵ_{\parallel} and ϵ_{\perp} are the corresponding parallel and perpendicular electric permittivities with respect to the director of the nematic molecules. In $\mathbb{R}^3 \setminus \Omega$, and consequently, in $\mathbb{R}^2 \setminus D$, we suppose vacuum with electric permittivity ϵ_0 . Assuming that the cross section D is orthogonal to \hat{y} , we define $\hat{n}(\alpha)$ in D by $\hat{n}(\alpha) = \sin(\alpha)\hat{x} + \cos(\alpha)\hat{z}$, where $(\hat{x}, \hat{y}, \hat{z})$ is the usual cartesian basis. Setting $\delta\epsilon = \epsilon_{\parallel} - \epsilon_{\perp}$, the second term of Eq. (3) is read as:

$$\frac{(\epsilon\vec{E}) \cdot \vec{E}}{2} = \begin{cases} \frac{(\delta\epsilon(\vec{\nabla}\phi \cdot \vec{n})^2 + \epsilon_{\perp}|\vec{\nabla}\phi|^2)}{2} & \vec{x} \in D, \\ \frac{\epsilon_0|\vec{\nabla}\phi|^2}{2} & \vec{x} \in \mathbb{R}^2 \setminus D. \end{cases} \quad (5)$$

Therefore, the total Helmholtz free energy per unit length of the system is

$$F(\alpha, \theta, \phi) = F_L + F_E. \quad (6)$$

Assuming that the prime variables have dimensionless units by using the transformations $L = \rho_m^{-2/3}$, $x = x'L$, $\epsilon = \epsilon_0\epsilon'$, $\epsilon_{\parallel} = \epsilon_0\epsilon'_{\parallel}$, $\epsilon_{\perp} = \epsilon_0\epsilon'_{\perp}$, $\phi = q_*(\epsilon_0L)^{-1}\phi'$, $\vec{E}' = -\vec{\nabla}'\phi'$, $F_0 = (q_*)^2(\epsilon_0L^2)^{-1}$, $F(\alpha, \theta, \phi) = F_0F'(\alpha', \theta', \phi')$, the dimensionless coefficients $f_1 = \rho_s F_0^{-1}$, $f_2 = KF_0^{-1}$, $f_3 = \lambda F_0^{-1}$ and dropping the prime symbols for simplicity, F_L and F_E can be written as follows (for more details, see Appendix A):

$$F_L = \int_D (f_1|\vec{\nabla}\theta|^2 + f_2|\vec{\nabla}\alpha|^2 + f_3(\hat{n} \cdot \vec{\nabla}\theta)^2) d^2x, \quad (7)$$

$$F_E = \int_D \phi d^2x - \int_{\mathbb{R}^2} \left(\frac{(\epsilon\vec{E}) \cdot \vec{E}}{2} \right) d^2x. \quad (8)$$

The dimensionless Helmholtz free energy per unit length can be inferred by inserting Eqs. (7)–(8) into Eq. (6).

2.2. Ginzburg–Landau equations

Firstly, the electric potential satisfies Laplace equation in $\mathbb{R}^2 \setminus D$:

$$\nabla^2\phi = 0. \quad (9)$$

Meanwhile in D , we look for the critical points of the dimensionless version of Eq. (6) in terms of (θ, ϕ, α) . Introducing the dimensionless factors $\bar{\epsilon} = \delta\epsilon\epsilon_{\perp}^{-1}$, $g_1 = f_1^{-1}f_3$, $g_2 = (2f_2)^{-1}f_3$, $g_3 = (4f_2)^{-1}\delta\epsilon$ and defining the following matrices:

$$\mathcal{A}(\alpha) = \begin{pmatrix} 1 + g_1 \sin^2 \alpha & \frac{g_1 \sin 2\alpha}{2} \\ \frac{g_1 \sin 2\alpha}{2} & 1 + g_1 \cos^2 \alpha \end{pmatrix}, \quad (10)$$

$$\mathcal{B}(\alpha) = \begin{pmatrix} \sin 2\alpha & \cos 2\alpha \\ \cos 2\alpha & -\sin 2\alpha \end{pmatrix}, \quad (11)$$

$$\mathcal{C}(\alpha) = \begin{pmatrix} 1 + \bar{\epsilon} \sin^2 \alpha & \frac{\bar{\epsilon} \sin 2\alpha}{2} \\ \frac{\bar{\epsilon} \sin 2\alpha}{2} & 1 + \bar{\epsilon} \cos^2 \alpha \end{pmatrix}, \quad (12)$$

the corresponding Ginzburg–Landau equations, obtained with standard variational calculus, are given by

$$\vec{\nabla} \cdot (\mathcal{A}(\alpha)\vec{\nabla}\theta) = 0, \quad (13)$$

$$\vec{\nabla} \cdot (\mathcal{C}(\alpha)\vec{\nabla}\phi) = -\frac{1}{\epsilon_{\perp}}, \quad (14)$$

$$\nabla^2\alpha - g_2\vec{\nabla}\theta^T\mathcal{B}(\alpha)\vec{\nabla}\theta + g_3\vec{\nabla}\phi^T\mathcal{B}(\alpha)\vec{\nabla}\phi = 0. \quad (15)$$

As we can see, Eq. (13) is the conservation law for the superfluid current $\vec{J}_s \propto \vec{\nabla}\theta$. Besides, Eq. (14) represents a modified Gauss Law for the system. Finally, Eq. (15) is a non linear equation for the nematic phase that shows the effects of the electric field and the superfluid current on the molecular alignment.

2.3. Effect of the superfluid current and the electric field on the Fréedericksz transition

The most used macroscopic model for neutral superfluids is based on the Gross–Pitaevskii theory [20], where the superfluid current is given by

$$\vec{J} = \frac{\hbar}{2m_*i} (\psi^*\vec{\nabla}\psi - \psi\vec{\nabla}\psi^*), \quad (16)$$

where $(*)$ denotes complex conjugation. In addition, $\hbar(m_*)^{-1}$ is proportional to the stiffness of the neutral superfluid. For the homogeneous case $\psi = \sqrt{n_0}e^{i\theta}$, where $|\psi|^2 = n_0$ is the mean density of superfluid particles. Hence, Eq. (16) becomes

$$\vec{J} = \frac{\hbar n_0 \vec{\nabla}\theta}{m_*}. \quad (17)$$

In order to understand the Fréedericksz transition for nematic superfluids, and inspired on the known fact in Eq. (17), we consider a particular solution of Eqs. (13)–(15) without circulation of the superfluid current

$$\oint_C \vec{J} \cdot \vec{dl} \propto \oint_C \vec{\nabla}\theta \cdot \vec{dl} = 0 \quad (18)$$

around a closed loop C . The superfluid current can be related to the electric field since $\vec{\nabla} \times \vec{E} = 0$ and then $\oint_C \vec{E} \cdot \vec{dl} = 0$. For this case, and comparing the matrix elements in Eqs. (10), (12), we can set that the superfluid phase θ and the electric potential ϕ are related by the following identity:

$$\theta = \frac{\bar{\epsilon}}{g_1}\phi. \quad (19)$$

Thus, using that $\rho_0 = \epsilon_{\perp}^{-1}(1 - \bar{\epsilon}g_1^{-1})^{-1}$, $b = g_3 - g_2(\bar{\epsilon}g_1^{-1})^2$, Eqs. (13)–(15) can be reduced to the following system of equations:

$$\nabla^2\phi = -\rho_0, \quad (20)$$

$$\nabla^2\alpha + b\vec{\nabla}\phi^T\mathcal{B}(\alpha)\vec{\nabla}\phi = 0. \quad (21)$$

The substitution given by Eq. (19) and Eq. (20) states that a particular solution for the superfluid phase and the electric potential satisfy Poisson equation. The previous relation produces an irrotational solution for these quantities. Furthermore, Eq. (21) suggests that the non circulating profile of the superfluid current can be added to the effects of the electric field on the nematic phase of the molecules. Hence, a Fréedericksz transition can take place on the nematic molecules, for suitable values of b , due to the influence of the electric field and the superfluid current. For a physical interpretation of these quantities, with $b_S = \bar{\epsilon}^2\rho_s^2(2K\lambda)^{-1}$ and $b_N = F_0\delta\epsilon(4K)^{-1}$, we rewrite b as follows:

$$b = b_N - b_S. \quad (22)$$

Here, b_S is a parameter that depends on the mean density of superfluid particles ρ_s and the coupling between nematic and superfluid effects λ . In addition, b_N is a parameter that depends on the electric anisotropy of the system, which appears in a pure nematic situation [18]. The previous decomposition in Eq. (22) clearly shows a crucial difference between nematic superfluid systems and its pure nematic counterpart, where the electric anisotropy is the main factor that determines the critical electric field, and subsequently, the Fréedericksz transition.

In the next section, we analyze the existence of a Fréedericksz transition in two different situations: When \vec{E} is a uniform electric field and when \vec{E} is a radial electric field produced by the internal charges of the sample. In particular, for the case of the uniform field, we will distinguish two possible cases depending on whether the cross section D is a disk or a slab. For the radial

field we analyze only the case when the section D is an annular domain. We also illustrate with Figs. (2–5) the behavior of the transition, via a graphical representation of $\hat{n}(\alpha)$, and the general threshold $|E|$ for different values of the ratio $b_S b_N^{-1}$.

3. Uniform electric field

In this section, we take a uniform electric field applied on the sample of the form $\vec{E}_a = E_1 \hat{x} + E_2 \hat{z}$, where E_1 and E_2 are given parameters. Throughout this section we consider valid the assumption expressed by Eq. (19). Consequently, we are focused to study the system given by Eqs. (20)–(21). Assuming that $\rho_0 \ll 1$, we have that $\vec{E} = \vec{E}_a$ is a solution for Eqs. (9) and (20). Thus, Eq. (21) becomes:

$$\nabla^2 \alpha + b \{(E_1^2 - E_2^2) \sin 2\alpha + 2E_1 E_2 \cos 2\alpha\} = 0, \quad (23)$$

which has a similar form to the expression shown in [21] for uniaxial nematic liquid crystals.

Let ω be the angle between the electric field \vec{E} and the unitary vector \hat{z} , i.e., $E_1 = |\vec{E}| \sin \omega$ and $E_2 = |\vec{E}| \cos \omega$. It is easy to check that $E_1^2 - E_2^2 = -|\vec{E}|^2 \cos 2\omega$ and $2E_1 E_2 = |\vec{E}|^2 \sin 2\omega$. Thus, Eq. (23) becomes

$$\nabla^2 \alpha + b |\vec{E}|^2 \sin 2(\omega - \alpha) = 0,$$

being $\gamma = \omega - \alpha$ the angle of the deviation between the electric field \vec{E} and the director \hat{n} . Hence, we obtain the following equation for $\gamma(\vec{x})$:

$$-\nabla^2 \gamma + b |\vec{E}|^2 \sin 2\gamma = 0. \quad (24)$$

In the subsections below, we analyze the existence of Fréedericksz transitions in two possible cross sections D .

3.1. General computation of a Fréedericksz threshold by using the first positive eigenvalue of the Laplacian

We begin with Eq. (24), where $\gamma \in L^2(D)$. Multiplying Eq. (24) by γ on both sides of the equality and integrating by parts in D , we have

$$\int_D (\gamma \nabla^2 \gamma - b |\vec{E}|^2 \gamma \sin 2\gamma) d^2x = 0, \\ \int_{\partial D} \gamma \vec{\nabla} \gamma \cdot \vec{dS} + \int_D (-|\vec{\nabla} \gamma|^2 - b |\vec{E}|^2 \gamma \sin 2\gamma) d^2x = 0.$$

Then, Dirichlet or Neumann boundary conditions produce that the first term of the previous equality vanishes, and this leads us to the following equality:

$$\|\vec{\nabla} \gamma\|_{L^2(D)}^2 = \int_D |\vec{\nabla} \gamma|^2 d^2x = \int_D -b |\vec{E}|^2 \gamma \sin 2\gamma d^2x. \quad (25)$$

Changing \hat{n} by $-\hat{n}$, if needed, we can assume that $\gamma \in (0, 2^{-1}\pi)$ and thus we have $\sin 2\gamma > 0$. With this assumption on Eq. (25), in which we shall consider $0 > b = -|b|$, we derive a bound for the electric field of the form

$$\|\vec{\nabla} \gamma\|_{L^2(D)}^2 = |b| |\vec{E}|^2 \int_D \gamma \sin 2\gamma d^2x \\ \leq |b| |\vec{E}|^2 \int_D |\gamma \sin 2\gamma| d^2x \\ \leq |b| |\vec{E}|^2 \int_D 2|\gamma|^2 d^2x \\ = 2|b| |\vec{E}|^2 \|\gamma\|_{L^2(D)}^2. \quad (26)$$

Since we are looking for a non trivial solution $\forall \gamma \in L^2(D)$, we obtain a bound that depends on the first positive eigenvalue of the

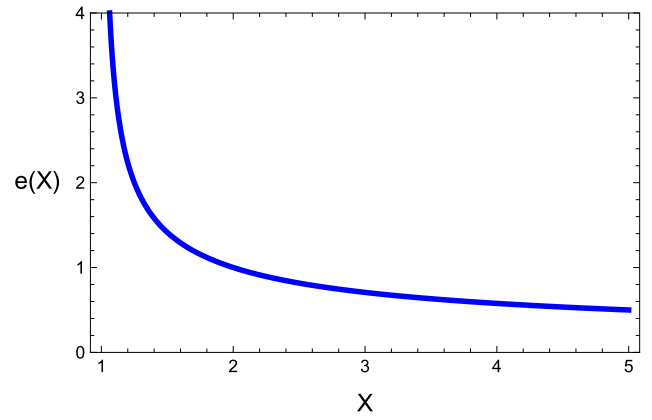


Fig. 1. Behavior of the effective Fréedericksz threshold $e(X)$ in the case $\gamma \in (0, 2^{-1}\pi)$ and $b < 0$.

Laplacian Λ_1 , with the corresponding boundary conditions [10]:

$$\Lambda_1 \leq \frac{\|\vec{\nabla} \gamma\|_{L^2(D)}^2}{\|\gamma\|_{L^2(D)}^2}. \quad (27)$$

Therefore, applying Eq. (27) into Eq. (26), we prove that the Fréedericksz threshold for the molecular alignment can be expressed as a condition for the electric field:

$$|\vec{E}|^2 \geq \frac{\Lambda_1}{2|b|}. \quad (28)$$

In order to illustrate the behavior of the electric field, we take $\delta\epsilon > 0$, $X = b_S b_N^{-1}$ and the effective threshold function as $\sqrt{2|b_N| \Lambda_1^{-1} |\vec{E}|^2} := e^2(X) \geq \frac{1}{(X-1)}$.

From Fig. 1 we can see that the Fréedericksz threshold increases when b_S and b_N tend to be equal. In fact, if $X \rightarrow 1$ the value of the critical electric field is extremely large. In contrast, for $X \rightarrow +\infty$ the critical electric field decreases to zero. From a physical point of view, the value of this field for the transition increases when the non pure nematic effects are comparable in size with the classical ones in nematic liquid crystals. Besides, with a particular choice of the parameters related with nematicity and superfluidity, it is possible to diminish the size of the critical electric field. (For the case $b > 0$, $\gamma \in (2^{-1}\pi, \pi)$, see Appendix B).

3.2. Fréedericksz transition in an infinite slab

In this subsection we consider an infinite slab $\Omega := \{(x, y, z) : 0 \leq x \leq d\}$ with cross section $D := \{(x, z) : 0 \leq x \leq d\}$ and an electric field \vec{E}_a . With the translational symmetry on the \hat{z} direction for the parameter α , i.e., $\alpha = \alpha(x)$, Eq. (24) becomes the following ordinary equation:

$$\frac{d^2 \gamma}{dx^2} - b |\vec{E}|^2 \sin 2\gamma = 0. \quad (29)$$

Next, we study Eq. (29) with Dirichlet or Neumann boundary conditions, both regarded as two suitable conditions for the crystals. The first one, $\gamma(0) = \gamma(d) = 0$, means that crystals are aligned in a given direction at the boundary. The second one, $\gamma'(0) = \gamma'(d) = 0$, means that the movement of crystals is smooth in the transverse direction to the boundary, and they stop when they approach it.

In order to get the Fréedericksz threshold, we apply the method presented in the previous subsection by computing the first eigenvalue of the one dimensional Laplacian in $[0, d]$, with both Dirichlet and Neumann boundary conditions. A straightforward computation gives $\Lambda_1 = \pi^2 d^{-2}$, which is the same for both

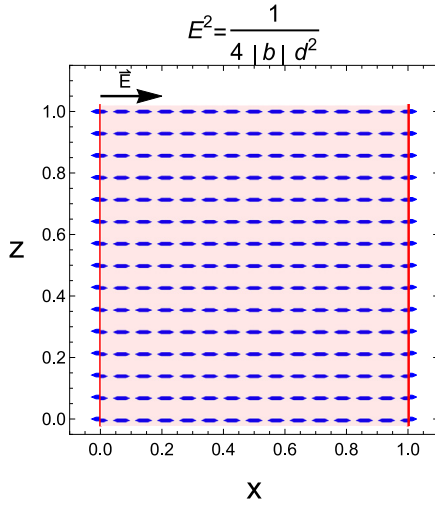


Fig. 2. Molecular alignment for Dirichlet boundary conditions $\alpha(0) = \alpha(1) = 2^{-1}\pi$ and below the threshold, in a unit square of the infinite slab with $d = 1$. We only observe the initial alignment.

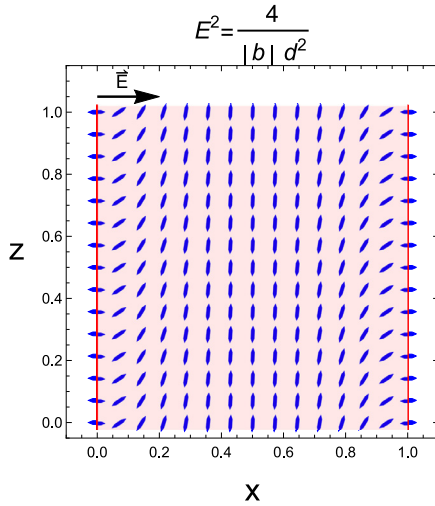


Fig. 3. Molecular alignment for Dirichlet boundary conditions $\alpha(0) = \alpha(1) = 2^{-1}\pi$ and above the threshold, in a unit square of the infinite slab with $d = 1$. We clearly notice the deviation on the molecular alignment due to the threshold.

problems. The previous result replaced into Eq. (28) implies that the critical electric field is

$$|\vec{E}|^2 \geq \frac{\pi^2}{2|b|d^2}. \quad (30)$$

As we stated before, by means of the quantity X we can compare Eq. (30) with the threshold in a pure nematic case. We notice that the magnitude of the critical electric field decreases when the difference in the contributions between both situations, nematicity (b_N) versus nematic superfluidity (b_S), increases ($X \gg 1$). In the following plots, we illustrate the molecular behavior as a function of the threshold. For this purpose, we sketch the numerical solution of Eq. (29) by using the shooting method (see Figs. 2 and 3).

3.3. Fréedericksz transition in a disk

In this subsection we consider $\Omega_d := \{(x, y, z) : x^2 + z^2 \leq d\}$, an infinite cylinder with cross section $D_d := \{(x, z) : x^2 + z^2 \leq d\}$.

In this geometry we expect $\alpha(x, z)$ due to the cylindrical symmetry. Consequently, we study the Fréedericksz transition for Eq. (24) with $\gamma(x, z)$, $b < 0$, $0 \leq \gamma \leq 2^{-1}\pi$ and considering both instances: Dirichlet boundary condition $\gamma|_{\partial D_d} = 0$, or Neumann condition $\frac{\partial \gamma}{\partial \eta}|_{\partial D_d} = 0$. We apply the technique described in Section 3.1 to find a threshold. First, Laplace equation in $D_d := \{0 \leq r \leq d, 0 \leq \varphi \leq 2\pi\}$ in polar coordinates, given by the coordinate transformations $x = r \sin \varphi$ and $z = r \cos \varphi$, can be written as follows:

$$\frac{1}{r}u_r + u_{rr} + \frac{1}{r^2}u_{\varphi\varphi} = -\Lambda u, \quad (31)$$

with Dirichlet boundary condition $u(d, \varphi) = 0$ or Neumann condition $u_r(d, \varphi) = 0$. We apply the separation of variables $u = R(r)\Phi(\varphi)$ into Eq. (31) in order to obtain Λ_1 provided with each boundary condition mentioned before. Then, it results that the eigenvalues for $\Phi(\varphi)$, imposing periodicity, are $\tilde{\mu}_k = k^2$, where $k \in \mathbb{N}_0$. In consequence, the equation for $R(r)$ is

$$r^2 R'' + rR' + (\Lambda r^2 - k^2)R = 0, \quad (32)$$

with the Dirichlet condition $R(d) = 0$ or the Neumann condition $R'(d) = 0$. In both situations we add the condition $R'(0) = 0$ in order to gain regularity of the solution at the origin. After the substitution $t = \sqrt{\Lambda}r$, Eq. (32) becomes the Bessel equation [22,23] with Dirichlet mixed condition $R(\sqrt{\Lambda}d) = R'(0) = 0$ or Neumann conditions $R'(0) = R'(\sqrt{\Lambda}d) = 0$. Here $J_k(t)$ is a Bessel function of order k . Using a numerical analysis for the first zero t_k of $J_k(t)$ and the first zero of their derivative t'_k , we deduce that the first positive eigenvalue Λ_1 of the Laplacian with Dirichlet condition in the disk is given by $\Lambda_1 = t_0^2 d^{-2}$, where $J_0(t_0) = 0$. Meanwhile, with Neumann condition we get $\Lambda_1 = t_2'^2 d^{-2}$, where $J_2'(t_2') = 0$. As a summary, the threshold for the Dirichlet condition is

$$|\vec{E}|^2 \geq \frac{t_0^2}{2|b|d^2} \quad (33)$$

and for the Neumann condition is

$$|\vec{E}|^2 \geq \frac{t_2'^2}{2|b|d^2}. \quad (34)$$

We observe from Eqs. (30), (33), (34) that the geometry influences the first positive eigenvalue of the Laplacian on the samples mentioned before, and consequently the Fréedericksz transition on each of them. From Eqs. (33)–(34) we also notice that the boundary conditions modify the critical electric field for the redirection of the molecular alignment. We display two graphics that sketch the molecular behavior above and below the threshold. We plot the solution for Eq. (24), which we find by performing a combination between the finite element method and a third order approximation of the sine function (see Figs. 4 and 5).

4. Radial electric field

In this section we explore a Fréedericksz type threshold, when the sample of nematic superfluid crystals is a long hollow cylinder along the \hat{y} axis, $\Omega_\varepsilon := \{(x, y, z) : \varepsilon^2 \leq x^2 + z^2 \leq 1\}$, with cross section $R_\varepsilon := \{(x, z) : \varepsilon^2 \leq x^2 + z^2 \leq 1\}$. With this in mind, we are concerned about the effects in the molecular alignment produced by a radial electric field, generated by the internal charges of the sample, with charge density ρ_0 .

According to the reduced system given by Eqs. (20)–(21), written in polar coordinates (r, φ) as the case of the disk, the electric field in Ω_ε can be calculated by applying Gauss Law [19]:

$$\vec{E} = \frac{\rho_0(r^2 - \varepsilon^2)\hat{r}}{2r}, \quad (35)$$

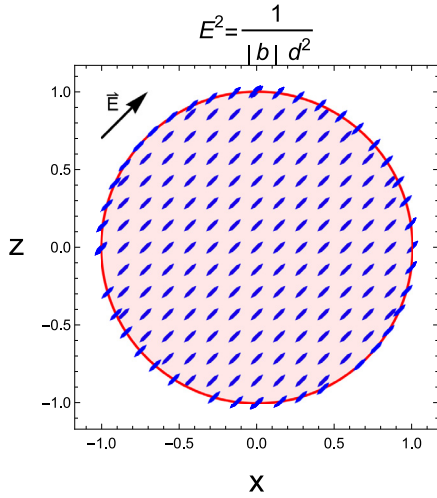


Fig. 4. Molecular alignment for Dirichlet boundary condition $\alpha(1) = 4^{-1}\pi$ and below the threshold, in a unit disk with $d = 1$. We only notice the initial molecular alignment.

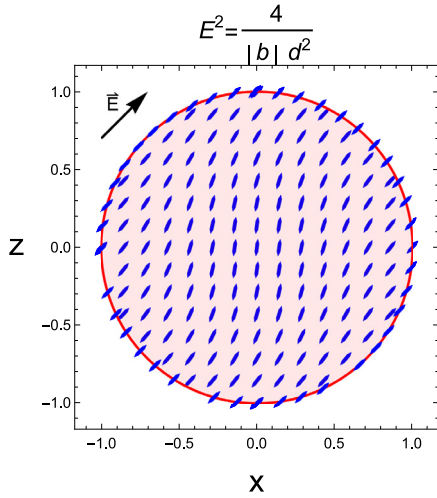


Fig. 5. Molecular alignment for Dirichlet boundary condition $\alpha(1) = 4^{-1}\pi$ and above the threshold, in a unit disk with $d = 1$. We clearly notice the deviation on the molecular alignment due to the threshold.

where $\hat{r} = \sin \varphi \hat{x} + \cos \varphi \hat{z}$. Then, replacing Eq. (35) in Eq. (21) and setting $g^\varepsilon(r) := (rE(r))^2$, we deduce the following equation for the nematic phase α :

$$r^2 \alpha_{rr} + r \alpha_r + \alpha_{\varphi\varphi} + b g_r^\varepsilon(r) \sin 2(\varphi - \alpha) = 0. \quad (36)$$

With the change of variables $r = e^{-t}$, Eq. (36) becomes

$$\alpha_{tt} + \alpha_{\varphi\varphi} + b g_r^\varepsilon(e^{-t}) \sin 2(\varphi - \alpha) = 0 \quad (37)$$

posed in $D_\varepsilon = [0, m_\varepsilon] \times [0, 2\pi]$, where $m_\varepsilon = \ln(1/\varepsilon)$. Setting $u = \varphi - \alpha$, Eq. (37) yields the following equation in the variables $(t, \varphi) \in D_\varepsilon$:

$$\nabla^2 u - b g^\varepsilon(e^{-t}) \sin 2u = 0. \quad (38)$$

Next, we impose periodicity in the nematic phase and we assume that the molecules are aligned in the radial direction at ∂R_ε . Hence, we apply the following boundary conditions at ∂D_ε :

$$u(t, \varphi) = u(t, \varphi + 2\pi), \quad (39)$$

$$u(t, \varphi)|_{\partial D_\varepsilon} = 0. \quad (40)$$

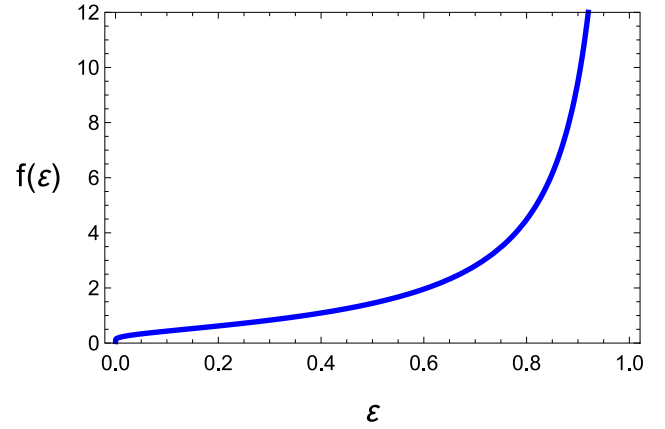


Fig. 6. Behavior of the effective type Fréedericksz threshold $f(\varepsilon)$ as a function of the inner radius ε . The previous plot states that the Fréedericksz threshold in this sample decreases when the inner radius of the hollow cylinder decreases, converging to the case of a disk.

Multiplying by u , integrating on D_ε and using integration by parts, we obtain

$$0 = \iint_{D_\varepsilon} |\vec{\nabla} u|^2 dt d\varphi + b \iint_{D_\varepsilon} g^\varepsilon(e^{-t}) u \sin 2u dt d\varphi \quad (41)$$

where the boundary term vanishes due to boundary conditions in Eqs. (39)–(40).

Assuming $0 \leq u \leq 2^{-1}\pi$, we thus have $u \sin 2u \geq 0$, and since $g^\varepsilon(s) \geq 0$ we conclude that the second term in Eq. (41) is non negative. Since we are looking for non trivial solutions, we assume that $b < 0$. Hence, we can write Eq. (41) as follows:

$$\iint_{D_\varepsilon} |\vec{\nabla} u|^2 dt d\varphi = |b| \iint_{D_\varepsilon} g^\varepsilon(e^{-t}) u \sin 2u dt d\varphi$$

which leads to the estimate

$$\Lambda_\varepsilon \|u\|_{L^2(D_\varepsilon)}^2 \leq 2|b| \|g^\varepsilon\|_{L^\infty(D_\varepsilon)} \|u\|_{L^2(D_\varepsilon)}^2, \quad (42)$$

where Λ_ε is the first positive eigenvalue of the Laplacian in D_ε , and u is orthogonal to the constant solutions in $L^2(D_\varepsilon)$. A straightforward calculation shows that $\Lambda_\varepsilon = \pi^2(\ln \varepsilon)^{-2}$, and finally from Eq. (42) the Fréedericksz threshold is

$$\|r\vec{E}(r)\|_{L^\infty(R_\varepsilon)}^2 \geq \frac{\pi^2}{2|b|(\ln \varepsilon)^2}. \quad (43)$$

The threshold presented in Eq. (43), considering the expression for the electric field inside the sample in Eq. (35), shows that molecules remain aligned with the radial direction when the charge density exceeds a certain value. This magnitude depends on an intrinsic parameter and the internal radius of the long hollow cylinder. Moreover, when $\varepsilon \rightarrow 0$ we obtain a trivial threshold for a disk, and molecules remain aligned with the radial direction of the electric field. A similar threshold can be derived if we take $2^{-1}\pi \leq u \leq \pi$ and $b > 0$. The behavior of $\sqrt{2|b|}\pi^{-1} \|r\vec{E}(r)\|_{L^\infty(R_\varepsilon)} := f(\varepsilon) = |\ln \varepsilon|^{-1}$ is described by Fig. 6.

5. Conclusions

In this article we present a model for the response of a nematic inhomogeneous superfluid material in presence of an electric field. This model consists of a set of three equations that express the coupling of the nematic phase, the superfluid phase and the electric potential. This system can be reduced to two equations by relating the superfluid phase and the electric potential, by

taking into account a particular solution for the Ginzburg–Landau equations without circulation. Consequently, we observe that a non trivial solution for the nematic phase is influenced by a threshold that depend on the electric field and the superfluid current. We take into account special instances with possible experimental applications due to their simplicity, that includes both the infinite slab and a cylinder when the electric field is uniform. We also take a hollow cylinder when the electric field is produced by the internal charges of the sample. Here, we notice that the Fréedericksz threshold is determined by the geometry of the system, the boundary conditions and the possible values of an intrinsic parameter that could be fixed experimentally. We also show that the Fréedericksz thresholds can be obtained by applying the notions of the first positive eigenvalue of the Laplacian for each problem, given Dirichlet or Neumann boundary conditions, on an arbitrary domain. Since it is easier to find bounds for the first eigenvalue than to get some special solution, the previous method appears to be a useful wide-range tool.

CRedit authorship contribution statement

Diego García Ovalle: Conceptualization, Methodology, Formal analysis, Writing - original draft. **Juan Pablo Borgna:** Conceptualization, Methodology, Formal analysis, Writing - review & editing. **Mariano De Leo:** Conceptualization, Methodology, Formal analysis, Writing - original draft, Writing - review & editing, Software.

Declaration of competing interest

The authors declare that they have no known competing financial interests or personal relationships that could have appeared to influence the work reported in this paper.

Appendix A. Dimensionless version of the Helmholtz free energy

We start from Eq. (6) and the following substitutions $x = Lx'$, $\epsilon = \epsilon_0\epsilon'$, $\phi = q_*\phi'(\epsilon_0L)^{-1}$, $\vec{E}' = -\vec{\nabla}\phi'$, $\alpha = \alpha'$, $\theta = \theta'$, where the prime symbols indicate dimensionless quantities and L is the unknown typical length of the system. Then, integrating on the dimensionless domain Ω' , we find that

$$\begin{aligned}
 F &= \int_{\Omega'} L^2 \left\{ q_* \rho_m^2 \left(\frac{q_*}{\epsilon_0 L} \right) \phi' + \frac{\rho_s}{L^2} |\vec{\nabla}\theta'|^2 + \frac{K}{L^2} |\vec{\nabla}\alpha'|^2 \right\} d^2x' \\
 &+ \int_{\Omega'} L^2 \left\{ \frac{\lambda}{L^2} (\hat{n} \cdot \vec{\nabla}\theta')^2 \right\} d^2x' \\
 &- \int_{\mathbb{R}^2} \left(\frac{q_*^2}{\epsilon_0^2 L^2} \right) \frac{L^2 (\epsilon_0 \epsilon' \vec{E}') \cdot \vec{E}'}{2L^2} d^2x' \\
 &= \int_{\Omega'} \left\{ \left(\frac{q_*^2 \rho_m^2 L}{\epsilon_0} \right) \phi' + \rho_s |\vec{\nabla}\theta'|^2 + K |\vec{\nabla}\alpha'|^2 \right\} d^2x' \\
 &+ \int_{\Omega'} \lambda (\hat{n} \cdot \vec{\nabla}\theta')^2 d^2x' - \int_{\mathbb{R}^2} \left(\frac{q_*^2}{\epsilon_0 L^2} \right) \frac{(\epsilon' \vec{E}') \cdot \vec{E}'}{2} d^2x'.
 \end{aligned}$$

Defining $F = F_0 F'$, where $F_0 = (q_*^2)(\epsilon_0 L^2)^{-1}$, we inferred that

$$\begin{aligned}
 F' &= \int_{\Omega'} \left\{ \rho_m^2 L^3 \phi' + \frac{\rho_s}{F_0} |\vec{\nabla}\theta'|^2 + \frac{K}{F_0} |\vec{\nabla}\alpha'|^2 \right\} d^2x' \\
 &+ \int_{\Omega'} \left\{ \frac{\lambda}{F_0} (\hat{n} \cdot \vec{\nabla}\theta')^2 \right\} d^2x' - \int_{\mathbb{R}^2} \frac{(\epsilon' \vec{E}') \cdot \vec{E}'}{2} d^2x'.
 \end{aligned}$$

Finally, with $\rho_m^2 = L^{-3}$, the dimensionless coefficients $f_1 = \rho_s F_0^{-1}$, $f_2 = K F_0^{-1}$, $f_3 = \lambda F_0^{-1}$ and dropping the prime symbols for simplicity, Eqs. (7)–(8) hold.

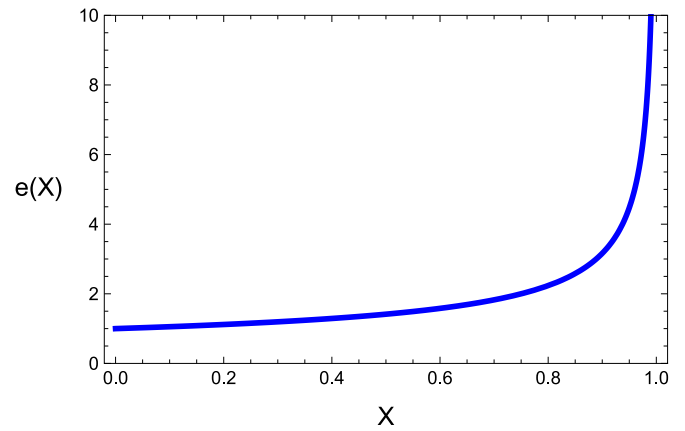


Fig. 7. Behavior of the effective Fréedericksz threshold $e(X) = (X - 1)^{-1/2}$, as a function of $X = b_S b_N^{-1}$, for $\delta\epsilon > 0$ in the case $\gamma \in (2^{-1}\pi, \pi)$ and $b > 0$.

Appendix B. Preliminaries for the graphical analysis of the critical electric field

In order to study the behavior of the general Fréedericksz threshold in Eq. (28), we take the effective function:

$$\frac{2b_N |\vec{E}|^2}{\Lambda_1} = e^2 \left(X = \frac{b_S}{b_N} \right) = \frac{1}{|1 - X|}. \tag{B.1}$$

if $\delta\epsilon > 0$. Then, equality (25) can be written as follows:

$$e^2 \geq \frac{1}{|1 - X|}. \tag{B.2}$$

From Eq. (B.2), we distinguish two cases for the effective critical field: if $X < 1$ ($2^{-1}\pi \leq \gamma \leq \pi$ and $b > 0$), Eq. (B.2) becomes:

$$|e| \geq \frac{1}{\sqrt{1 - X}} \tag{B.3}$$

and we recover the pure nematic case if $X \rightarrow 1$. Additionally, if $X > 1$ ($0 \leq \gamma \leq 2^{-1}\pi$ and $b < 0$), Eq. (B.2) leads to (see Fig. 7):

$$|e| \geq \frac{1}{\sqrt{X - 1}}. \tag{B.4}$$

References

- [1] D. Andrienko, Introduction to liquid crystals, J. Molecular Liquids 267 (2018) 520–541, Special Issue Dedicated to the Memory of Professor Y. Reznikov. <http://dx.doi.org/10.1016/j.molliq.2018.01.175>.
- [2] V. Fréedericksz, V. Zolina, Forces causing the orientation of an anisotropic liquid, Trans. Faraday Soc. 29 (1933) 919930, <http://dx.doi.org/10.1039/TF9332900919>.
- [3] P. Collings, M. Hird, Introduction to Liquid Crystals: Chemistry and Physics, Liquid Crystals Book Series, CRC Press, 2017.
- [4] D.V. Makarov, A.N. Zakhlevnykh, Tricritical phenomena at the Fréedericksz transition in ferronematic liquid crystals, Phys. Rev. E 81 (2010) 051710, <http://dx.doi.org/10.1103/PhysRevE.81.051710>.
- [5] M. Konerack, V. Zvirov, P. Kopcansk, J. Jadzyn, G. Czechowski, B. Zywuicki, Study of the magnetic fredericksz transition in ferronematics, J. Magn. Magn. Mater. 157–158 (1996) 589–590, European Magnetic Materials and Applications Conference. [http://dx.doi.org/10.1016/0304-8853\(95\)01196-X](http://dx.doi.org/10.1016/0304-8853(95)01196-X).
- [6] M.Y. Kagan, Modern trends in Superconductivity and Superfluidity, Lecture Notes in Physics, Springer Netherlands, 2013.
- [7] J. Zaanen, Z. Nussinov, S. Mukhin, Duality in 2+1D quantum elasticity: superconductivity and quantum nematic order, Ann. Physics 310 (1) (2004) 181–260, <http://dx.doi.org/10.1016/j.aop.2003.10.003>.
- [8] G. Zhu, J. Koch, I. Martin, Nematic quantum liquid crystals of bosons in frustrated lattices, Phys. Rev. B 93 (2016) 144508, <http://dx.doi.org/10.1103/PhysRevB.93.144508>.

- [9] G. Assanto, *Nematicons: Spatial Optical Solitons in Nematic Liquid Crystals*, in: *Wiley Series in Pure and Applied Optics*, Wiley, 2012.
- [10] J.P. Borgna, P. Panayotaros, D. Rial, C.S.F. de la Vega, Optical solitons in nematic liquid crystals: model with saturation effects, *Nonlinearity* 31 (4) (2018) 1535, <http://dx.doi.org/10.1088/1361-6544/aaa2e2>.
- [11] J.P. Borgna, P. Panayotaros, D. Rial, C.S.F. de la Vega, Optical solitons in nematic liquid crystals: Arbitrary deviation angle model, *Physica D* 408 (132448) (2020) <http://dx.doi.org/10.1088/1361-6544/aaa2e2>.
- [12] D.G. Barci, R.V. Clarim, N.L. Silva Júnior, Vortex and disclination structures in a nematic-superconductor state, *Phys. Rev. B* 94 (2016) 184507, <http://dx.doi.org/10.1103/PhysRevB.94.184507>.
- [13] S. Yonezawa, et al., Thermodynamic evidence for nematic superconductivity in, *Nat. Phys.* 13 (2017) <http://dx.doi.org/10.1038/nphys3907>.
- [14] R. Tao, Y.-J. Yan, X. Liu, Z.-W. Wang, Y. Ando, Q.-H. Wang, T. Zhang, D.-L. Feng, Direct visualization of the nematic superconductivity in $\text{Cu}_x\text{Bi}_2\text{Se}_3$, *Phys. Rev. X* 8 (2018) 041024, <http://dx.doi.org/10.1103/PhysRevX.8.041024>.
- [15] E. Berg, E. Fradkin, S.A. Kivelson, Theory of the striped superconductor, *Phys. Rev. B* 79 (2009) 064515, <http://dx.doi.org/10.1103/PhysRevB.79.064515>.
- [16] D.G. Barci, E. Fradkin, Role of nematic fluctuations in the thermal melting of pair-density-wave phases in two-dimensional superconductors, *Phys. Rev. B* 83 (2011) 100509, <http://dx.doi.org/10.1103/PhysRevB.83.100509>.
- [17] H. F. London, The electromagnetic equations of the supraconductor, *Proc. R. Soc. Lond. Ser. A Math. Phys. Eng. Sci.* 149 (866) (1935) 71–88, <http://dx.doi.org/10.1098/rspa.1935.0048>.
- [18] I. Khoo, *Liquid Crystals*, in: *Wiley Series in Pure and Applied Optics*, Wiley Interscience, 2007.
- [19] D. Griffiths, *Introduction to Electrodynamics*, Prentice Hall, 1999.
- [20] E. Sonin, *Dynamics of Quantised Vortices in Superfluids*, Cambridge University Press, 2016, <http://dx.doi.org/10.1017/CBO9781139047616>.
- [21] E. Priestley, P. Wojtowicz, P. Sheng, *Introduction to Liquid Crystals*, Plenum Press New York And London, 1975.
- [22] F. Bowman, *Introduction to Bessel Functions*, in: *Dover Books on Mathematics*, Dover Publications, 1958.
- [23] G. Watson, *Introduction to Bessel Functions*, Cambridge University Press, 1922.